

ErasableMask: A Robust and Erasable Privacy Protection Scheme against Black-box Face Recognition Models

Sipeng Shen, Yunming Zhang, Dengpan Ye, *Member, IEEE*, Xiuwen Shi, Long Tang, Haoran Duan, Yueyun Shang, Zhihong Tian, *Senior Member, IEEE*

Abstract—While face recognition (FR) models have brought remarkable convenience in face verification and identification, they also pose substantial privacy risks to the public. Existing facial privacy protection schemes usually adopt adversarial examples to disrupt face verification of FR models. However, these schemes often suffer from weak transferability against black-box FR models and permanently damage the identifiable information that cannot fulfill the requirements of authorized operations such as forensics and authentication. To address these limitations, we propose ErasableMask, a robust and erasable privacy protection scheme against black-box FR models. Specifically, via rethinking the inherent relationship between surrogate FR models, ErasableMask introduces a novel meta-auxiliary attack, which boosts black-box transferability by learning more general features in a stable and balancing optimization strategy. It also offers a perturbation erasion mechanism that supports the erasion of semantic perturbations in protected face without degrading image quality. To further improve performance, ErasableMask employs a curriculum learning strategy to mitigate optimization conflicts between adversarial attack and perturbation erasion. Extensive experiments on the CelebA-HQ and FFHQ datasets demonstrate that ErasableMask achieves the state-of-the-art performance in transferability, achieving over 72% mean confidence in commercial FR systems. Moreover, ErasableMask also exhibits outstanding perturbation erasion performance, achieving over 90% erasion success rate.

Index Terms—Facial privacy, Adversarial example, Face recognition

I. INTRODUCTION

WITH the advancement of deep learning, face recognition (FR) technology has become deeply integrated into daily life [1]–[4]. Users frequently share personal facial images on social media platforms such as Twitter, Facebook, and LinkedIn, which provides great convenience for trusted authorities (TAs) in performing face verification. However, this convenience comes with significant privacy risks. Attackers can match these images with existing biometric databases

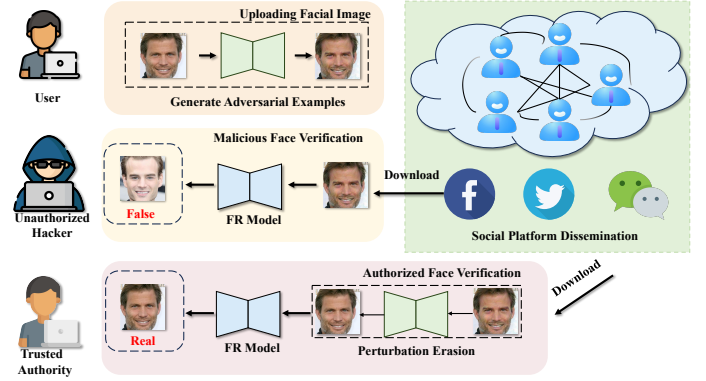


Fig. 1. ErasableMask protection scenario: Users generate protected faces and then publicly share them on social platforms. Unauthorized hackers fail to conduct face verification. However, trusted authority can utilize ErasableMask’s erasion module to obtain clean examples that are nearly identical to the original face, allowing to conduct face verification accurately.

to accurately identify individuals, facilitating serious criminal activities [5]. As a result, there is an urgent need for a robust scheme that can address the misuse and threats posed by FR technology while effectively preserving the usability of the information for TAs.

Existing adversarial examples [6]–[11] against FR models can serve as a feasible solution. However, they suffer from the following challenges: 1). **Existing schemes exhibit weak transferability towards strictly black-box FR models.** Some transferable adversarial example schemes have been proposed in recent year [12]–[16], which simply employ ensemble attack for all surrogate models. Unfortunately, this often leads to overfitting of the surrogate white-box models [17], resulting in weak transferability. In ensemble attacks, models often prioritize fitting the more easily attackable surrogate models before gradually adapting to the relatively harder-to-attack ones. This observation indicates an imbalance in the optimization process. Consequently, even if the ensemble attack loss converges, the model tends to overfit to the surrogate models and fails to learn robust and general features. This raises the question: *Can the model learn more robust and general features if it can learn in a stable and balancing attack strategy?* 2). **The adversarial performance permanently disrupts face verification of trusted authority for forensics and authentication.** The most obvious obstacle encountered by existing schemes is their permanently damage

Sipeng Shen, Yunming Zhang, Dengpan Ye, Xiuwen Shi, Long Tang, and Haoran Duan are with the Key Laboratory of Aerospace Information Security and Trusted Computing, Ministry of Education, School of Cyber Science and Engineering, Wuhan University. E-mail: {sipeng, zhangyunming, yedp, shixiuwen, l_tang, haoraod}@whu.edu.cn. Yueyun Shang is with School of Mathematics and Statistics, South-Central University for Nationalities, Wuhan 430070, P.R. China. E-mail: 36214001@qq.com. Zhihong Tian is with Cyberspace Institute of Advanced Technology, Guangzhou University, Guangdong Key Laboratory of Industrial Control System Security, and Huangpu Research School of Guangzhou University. E-mail: tianzhihong@gzhu.edu.cn. Sipeng Shen and Yunming Zhang contributed equally to this work. (Corresponding author: Dengpan Ye, Yueyun Shang.)

to the identifiable information present in the source faces. This severely hinders the ability of TAs to accurately perform face verification. Reversible Adversarial Examples (RAEs) can serve as one of potential strategies for TA's demands [18]–[21]. Most of them adopt a reversible data hiding strategy to fulfil recovery of original images [18], [19], [22]. However, RAEs exhibit several limitations. They fail to address the robustness of recovery that cannot tackle with various image process methods in real-world scenarios and overlook facial identity protection, leaving a gap in facial privacy protection scenarios. Additionally, existing RAEs typically combine pixel-level adversarial perturbations with separate data hiding techniques. This raises the question: *Would it be possible to design semantic perturbations in facial privacy protection scenarios that are inherently self-erasable?*

To resolve the questions mentioned above, we present a novel facial privacy protection scheme called ErasableMask, which utilizes facial attributes as conditions to generate transferable and erasable adversarial examples with strong robustness to tackle with various image process methods. Specifically, ErasableMask solves the above question through the following strategies:

To tackle with question 1. Existing studies have demonstrated that auxiliary learning can serve as a promising balancing strategy, which enhances generalization of the primary task by learning additional relevant features obtained in the sharing of features with auxiliary tasks [23], [24]. This motivates us to think about whether the model can learn a more transferable attack through this stable and balancing strategy, where attacking one specific surrogate FR model serves as a primary task and fine-grained fine-tuned the model with feedback from other surrogate FR models as auxiliary tasks. But there exists a question of how to transfer the strategy learned from the primary task to the auxiliary tasks, while also allowing the auxiliary tasks to provide beneficial feedback. Recently, meta-learning has been utilized to improve the optimization compatibility between different tasks [25], [26]. As a result, we introduce a novel meta-auxiliary attack to learn more robust and general features that boost transferability. Specifically, we split surrogate FR models into a primary task and several auxiliary tasks before each attack, then use the performance of auxiliary tasks in meta-test to further fine-grained fine-tuned optimization direction of the primary task in meta-train, which is a form of meta-learning with double gradient.

To tackle with question 2. One direct method to enable self-erasable capability is deploying a restorer, allowing it to be tightly coupled with the generator and trained end-to-end with it. However, there exists a problem that the clean-domain information in protected faces is severely damaged, resulting in a difficulty for restorer to obtain enough information that facilitate perturbation erasure. This inspires us to consider whether we can retain enough clean-domain information that can guide perturbation erasure. As a result, we employ a clean-domain information injection strategy which embeds additional source face information via a copy of generator to improve perturbation erasure performance. Moreover, the adversarial generation and erasure of semantic perturbations are a set of conflicting optimization objectives. And to tackle with

real-world transmission standards, ErasableMask also needs to hold robustness both in adversarial attack and perturbation erasure, which can be fulfilled by a differential noise pool [27]. Directly deploying this noise pool will undoubtedly increase the difficulty of training for this conflicting task. This prompts us to think about making the ErasableMask generator and restorer acquire adversarial, erasable, and robust capabilities step by step to mitigate conflicts. Thus, we adopt a three-stage curriculum learning [28] strategy. Specifically, we allow ErasableMask to solely focus on attribute modification strategy in stage 1 and deploy the noise pool in the last two phases (introducing robust adversarial example in stage 2 and robust perturbation erasure in stage 3).

To the best of our knowledge, ErasableMask is the first self-erasable facial privacy protection scheme. As shown in Fig. 1, ErasableMask strikes a balance between facial privacy protection and information usability. Compared with existing works in Table. I, ErasableMask supports self-erasable ability and strong robustness both in attack and recovery. Overall, ErasableMask makes the following contributions:

- 1) We design a meta-auxiliary attack strategy that balances attack stability and generalization. This strategy encourages the model to learn transferable features, significantly improving the attack performance on black-box face recognition (FR) systems.
- 2) We introduce a curriculum learning-based optimization scheme that progressively aligns adversarial attack objectives with perturbation erasure goals, mitigating the inherent conflicts between them and leading to step-wise improvement in both attack and erasure capability.
- 3) Extensive experiments demonstrate that ErasableMask achieves state-of-the-art performance across three dimensions: black-box transferability (average confidence over **72%** in commercial FR systems), perturbation erasure (**90%+** success rate in black-box scenarios), and robustness (minimal performance drop under common image transformations).

II. RELATED WORK

TABLE I
COMPARISON OF WORKS ON ADVERSARIAL EXAMPLES.

Scheme	Victim	Perturb	Recovery		Robustness	
			Combined	Self-erasable	Attack	Recovery
[29]	Class	Pixel	×	×	×	×
[30]	Class	Pixel	×	×	×	×
[19]	Class	Pixel	✓	×	×	×
[18]	Class	Pixel	✓	×	✓	×
[20]	Class	Pixel	×	✓	✓	×
[31]	FR	Pixel	×	×	×	×
[6]	FR	Pixel	×	×	×	×
[11]	FR	Semantic	×	×	×	×
[32]	FR	Semantic	×	×	×	×
ours	FR	Semantic	×	✓	✓	✓

FR: Face Recognition; **Class:** Classification

Pixel: Pixel-level perturbation; **Semantic:** Semantic-level perturbation.

Combined: Information hiding-based recovery; **Self-erasable:** optimization based.

Attack: Robustness for attack; **Recovery:** Robustness for recovery.

✓: means the scheme achieves this property; ×: means it does not.

A. Adversarial Examples

Many studies have shown that deep neural networks (DNNs) are highly vulnerable to adversarial examples. Depending

on the adversary's knowledge of the target model, these schemes can be categorized into black-box and white-box attacks [29], [30]. White-box attacks and query-based black-box attacks [8], which rely on knowledge of the target models, are limited in practical scenarios. Therefore, this paper mainly considers transfer-based black-box attacks [33]–[36], which aims at improving transferability without the knowledge of the target model. Although adversarial examples demonstrate extraordinary potential in attacking classification model, the unerasable adversarial performance inevitably prevent their applications in privacy protection scenarios.

Recently, a special type of adversarial example, Reversible adversarial examples (RAEs) have been of increasing interest. RAEs can mislead classification model and conduct recovery of origin images, which can server a promising solution for privacy protection. Most of them adopt additive perturbations along with reversible data hiding method [18], [19], [21], [22]. They either consider black-box attacks against classification models [18]–[20], or a gender protection scenario [21]. However, there is a gap both in facial privacy protection scenarios, where RAEs cannot support robust recovery that resist image process methods, and the self-erasable ability of semantic perturbations.

B. Adversarial Example against Face Recognition

Existing attacks against FR systems primarily fall into two categories: patch-based [7], [9] and perturbation-based [6], [8], [29], [30], [33], [37] attacks. Patch-based attacks, such as Adv-Hat [7], Adv-Makeup [17], and SOP [38], add noticeable patches to specific regions of facial images. However, this method significantly degrades image usability. In the other category, perturbation-based adversarial attacks can introduce more imperceptible noise on facial images. Moreover, most schemes against FR models tend to employ ensemble attacks simply without an in-depth insight in how to improve transferability. Recently, GMAA [32] improves black-box transferability by introducing a set of the target face with different poses, thus transforming the discrete target domain into a manifold one, which is more likely a data augmentation trick. Sibling-Attack [31] uses attacking AR models as an auxiliary task, generating additive adversarial perturbations through multi-task optimization. The strategy of Sibling-Attack is enlarging search space, and this additive perturbation will inevitably introduce noticeable noise on facial images. However, existing schemes lack considerations on how to improve transferability with an in-depth insight into the inherent relationship between FR models. Moreover, all of them cannot support recovery of source facial images, which hinders the authentication and management of TAs.

III. PROBLEM STATEMENT

In general, there are two kinds of adversarial examples against FR models, including untargated (dodging) and targated (impersonation) attacks. Numerous facial privacy protection schemes have been proposed [13], [14], [39] aiming at impersonation attacks. As a result, in this section, we formulate a facial privacy protection scenario based on impersonation attacks and provide a comprehensive description of the

abilities and goal of users, trusted authority, and unauthorized hackers.

A. Users' Ability and Goal

Users possess several facial images $x_{cov} \in \mathbb{R}^{h \times w}$, where \mathbb{R} denotes the real number field, and h , w denotes the height and width of the x_{cov} respectively. Users have no knowledge about the parameters or architecture of malicious FR models but can leverage a locally held facial privacy protection model to process x_{cov} , resulting in a protected image x_{adv} . In general, the protected face generation process can be expressed as the following formula:

$$\begin{aligned} \max_{x_{adv}} \quad & \mathcal{L}_{adv} = \mathcal{D}(FR(x_{adv}), FR(x_{target})) \\ \text{s.t.} \quad & \|x_{adv} - x_{cov}\|_p \leq \delta. \end{aligned} \quad (1)$$

where $\mathcal{D}(\cdot)$ denotes a distance function. $FR(\cdot)$ denotes a DNN-based FR model. x_{adv} denotes protected faces, x_{cov} denotes source face and x_{target} denotes target face. $\|x_{adv}, x_{cov}\|_p \leq \delta$ is utilized to quantify the visual similarity between x_{adv} and x_{cov} , where $\|\cdot\|_p$ means L_p norm.

B. Trusted Authorities' Ability and Goal

Trusted Authorities (TAs) represent platform managers, and need to conduct face verification in forensics scenarios. TAs can obtain the clean example x_{rec} through the restorer and conduct face verification through the FR model they hold. TAs are totally honest entities and would not deliver restorer and x_{rec} to UHs or other Users. Therefore, we redefine facial privacy protection scenario in erasion perspective. We present a formula for recovery example x_{rec} .

$$\begin{aligned} \min_{x_{rec}} \quad & \mathcal{L}_{erasion} = \mathcal{D}(FR(x_{rec}), FR(x_{target})) \\ \text{s.t.} \quad & \|x_{rec} - x_{cov}\|_p \leq \delta. \end{aligned} \quad (2)$$

In the process of erasion, we expect the erasion operation to eliminate the adversarial strength towards x_{target} to the greatest extent. We quantify the visual similarity between x_{rec} and x_{cov} through the function $\|x_{rec}, x_{cov}\|_p$.

C. Unauthorized Hackers' Ability and Goal

Unauthorized Hackers (UHs) can obtain facial images from online platforms and conduct malicious face verification. Based on their ability to defend against adversarial examples, we define the following two types:

Professional Unauthorized Hackers (PUHs): In this case, PUHs are experts in adversarial examples and face recognition, possessing the ability to fine-tune FR models and resist adversarial threats.

Regular Unauthorized Hackers (RUHs): In this case, They can only acquire FR models trained on large-scale data from the internet, or use commercial FR models.

IV. METHODOLOGY

As shown in Fig. 2, we built the ErasableMask framework using a conditional GAN architecture [40]. ErasableMask consists of a generator G , which is composed of an encoder G_{enc} , a perturbation encoder E_{adv} , and a decoder G_{dec} . A restorer R , and a discriminator D , which has two components including an attribute classifier D_{att} and a discriminator D_G .

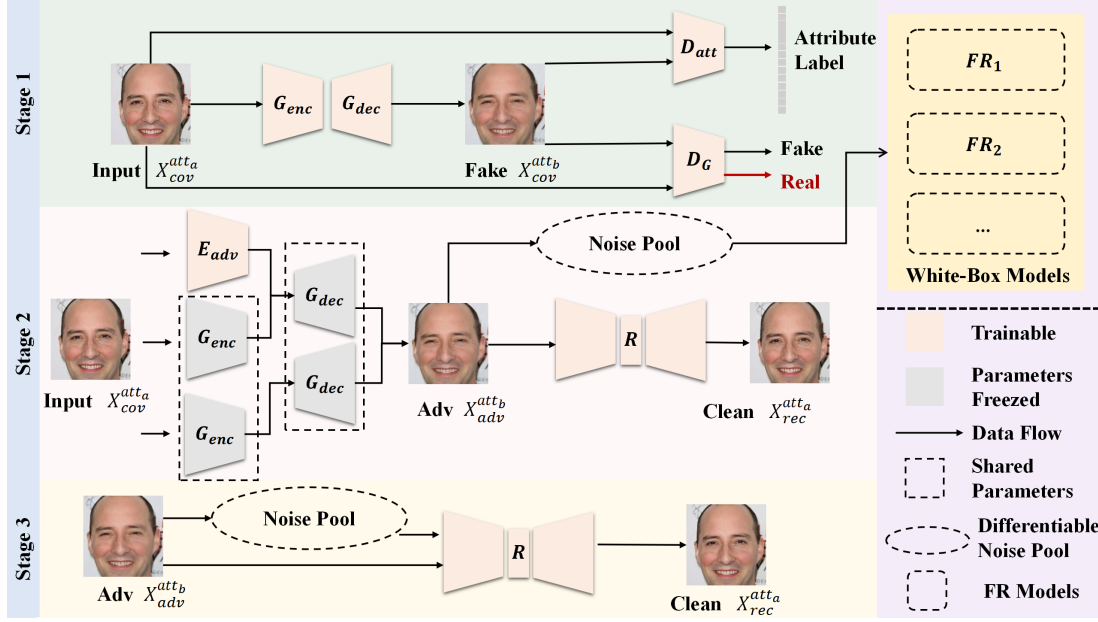


Fig. 2. Pipeline of ErasableMask: A three-stage curriculum learning is introduced to address optimization conflicts between adversarial and erasure performance. Stage 1: G_{enc} and G_{dec} learn an attribute modification strategy. Stage 2: E_{adv} and R are tightly coupled and trained end-to-end. Stage 3: The robustness and erasure capabilities of R are further strengthened.

A. Visual Identity-preserved Facial Attribute Manipulation

As input, the generator G first receives a clean domain facial image $x_{cov}^{att_a}$ with n -bit attribute label $att_a \in \{0, 1\}^n$ and a n -bit attribute label $att_b \in \{0, 1\}^n$ to generate a protected example $x_{adv}^{att_b}$. The discriminator D_G learns to distinguish the clean domain image $x_{cov}^{att_a}$ from the protected face $x_{adv}^{att_b}$. Correspondingly, the generator G learns to generate protected faces that match the real image distribution to deceive D_G .

$$\begin{aligned} \mathcal{L}_D &= -\log D_G(x_{cov}^{att_a}) - \log (1 - D_G(x_{adv}^{att_b})), \\ \mathcal{L}_G &= -\log (D_G(x_{adv}^{att_b})). \end{aligned} \quad (3)$$

To ensure that $x_{adv}^{att_b}$ retains the correct attributes in face, we employ the attribute constraint loss to effectively disentangle facial attribute information in high-dimensional feature space. By constraining $x_{adv}^{att_b}$ with the \mathcal{L}_{att}^G in attribute classifier D_{att} , we reduce the semantic difference between $x_{adv}^{att_b}$ and the target attributes att_b . The loss function can be formulated as:

$$\begin{aligned} \mathcal{L}_{att}^D &= \sum_{i=1}^n -att_{a_i} \log D_{att}(x_{cov}^{att_a}) \\ &\quad - (1 - att_{a_i}) \log (1 - D_{att}(x_{cov}^{att_a})), \\ \mathcal{L}_{att}^G &= \sum_{i=1}^n -att_{b_i} \log D_{att}(x_{adv}^{att_b}) \\ &\quad - (1 - att_{b_i}) \log (1 - D_{att}(x_{adv}^{att_b})). \end{aligned} \quad (4)$$

The encoder G_{enc} must ensure that the generated image retains as much of the facial content information from the source image $x_{cov}^{att_a}$ as possible, as the latent variable z needs to enable the decoder G_{dec} to reconstruct attribute-independent details for any attribute conditions. To achieve this, the reconstruction loss \mathcal{L}_{rec} is introduced.

$$\mathcal{L}_{rec} = \|G_{dec}(G_{enc}(x_{cov}^{att_a}), att_a) - x_{cov}^{att_a}\|_1, \quad (5)$$

where $\|\cdot\|_1$ represents the L_1 loss.

Algorithm 1 Meta-auxiliary Attack

Input: $x_{cov}^{att_a}$ (source image); $G(\cdot)$ (adversarial example generator); $FR_i \in \{FR_1, FR_2 \dots FR_K\}$ (surrogate FR models);

Output: best model parameters;

```

1: Initialization:  $\mathcal{L}_{FR_i}\{0\} = \mathcal{L}_{FR_i}\{1\} = 1$ ;
2: for  $i \in [0, Epoch]$  do
3:   for  $x_{cov}^{att_a} \in Dataset$  do
4:      $x_{adv}^{att_b} \leftarrow G(x_{cov}^{att_a}, att_b)$ ;
5:     for  $p \in [1, \dots, K]$  do
6:       Calculate  $\mathcal{L}_{FR_p}^{pri}$  with Eq. 9;
7:        $\theta'_E = \theta_E - lr \cdot \nabla_{\theta_E} \mathcal{L}_{FR_p}^{pri}(\theta_E)$ ;
8:       for  $q \in \{1, \dots, K\} \cap q \neq p$  do
9:          $x_{adv}^{att_b} \leftarrow G(x_{cov}^{att_a}, \theta'_E, att_b)$ ;
10:      end for
11:      Calculate  $\mathcal{L}_{FR_p}^{aux}$  with Eq. 10;
12:    end for
13:    Calculate  $\mathcal{L}_{adv}$  and update  $E_{adv}$  with Eq. 12;
14:  end for
15:  Calculate  $w_i(t)$  with Eq. 11;
16: end for
17: return best model parameters;
```

B. Meta-auxiliary Attack for Semantic Perturbations

Unlike pixel-level perturbations, ErasableMask achieves a more natural and realistic result for $x_{adv}^{att_b}$ by introducing semantic perturbations, as illustrated in Fig. 3. Specifically, G_{enc} and G_{dec} are well-trained under the constraints in section IV-A to generate naturally realistic attribute-modified images. On this basis, ErasableMask introduces a perturbation

encoder E_{adv} , which is initially set with parameters identical to G_{enc} . During training, E_{adv} applies semantic perturbations

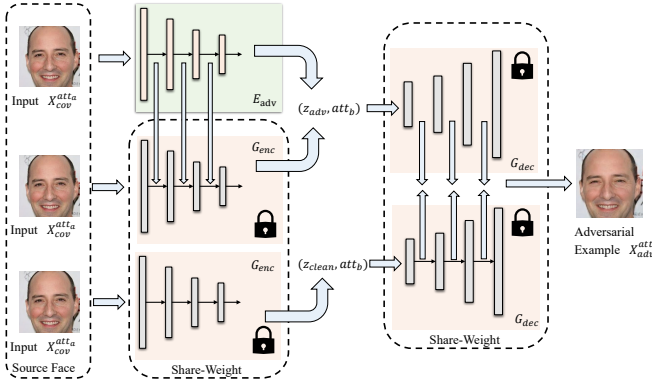


Fig. 3. Detailed framework of semantic perturbations and clean-domain information injection.

by fusing its each layer's outputs with each layer of G_{enc} 's output. Denoting the i -th layer of G_{enc} as G_{enc}^i and the i -th layer of E_{adv} as E_{adv}^i , where $i \in \{1, \dots, n\}$ for an encoder with n layers, the operations to the i -th layer of G_{enc} can be represented as:

$$\begin{aligned} ft_i &= G_{enc}^i(ft_{i-1}), \\ perb_i &= E_{adv}^i(perb_{i-1}), \\ fs_i &= \beta \cdot ft_i + (1 - \beta) \cdot perb_i. \end{aligned} \quad (6)$$

Specifically, both G_{enc} and E_{adv} take the clean example $x_{cov}^{att_a}$ as their input. The decoding process of G_{dec} is:

$$\begin{aligned} z_{adv} &= [fs_1, fs_2, \dots, fs_n], \\ x_{adv}^{att_b} &= G_{dec}(z_{adv}, att_b). \end{aligned} \quad (7)$$

To avoid $x_{adv}^{att_b}$ differing from $x_{cov}^{att_b}$ largely, a perturbation loss \mathcal{L}_{perb} is introduced.

$$\mathcal{L}_{perb} = \max(\sigma_1, \|x_{adv}^{att_b} - x_{cov}^{att_b}\|_2), \quad (8)$$

where $\sigma_1 \in (0, +\infty)$, and $\|\cdot\|_2$ represents the L_2 norm. In ErasableMask, σ_1 is set to 30.0. Particularly, $x_{cov}^{att_b}$ can be generated from $x_{cov}^{att_b} = G_{dec}(G_{enc}(x_{cov}^{att_a}), att_b)$.

To enable $x_{adv}^{att_b}$ to demonstrate adversarial performance, we need to employ a transferable attack strategy. However, the existing ensemble attack fails to learn general and robust features due to its unbalanced and unstable learning process. (weak transferability in our experiments). Motivated by this, we introduce a more stable and balancing attack strategy called meta-auxiliary attack, to fine-grained fine-tuned the optimization direction of E_{adv} via additional beneficial features from other surrogate models during each attack. The algorithm is demonstrated in Alg. 1. Specifically, before attacking a specific surrogate FR model, we split K white-box surrogate models $\{FR_i | i \in \{1, \dots, K\}\}$ into 1 primary task and $K - 1$ auxiliary tasks (All surrogate FR models take turns as primary task). For the convenience of description, we take surrogate model FR_A as an example, the rest surrogate models $\{FR_i | i \in \{1, \dots, K\} \cap i \neq A\}$ denote auxiliary tasks. Thereafter, we conduct meta-train in primary task:

$$\mathcal{L}_{FR_A}^{pri} = 1 - \cos[FR_A(x_{target}), FR_A(x_{adv}^{att_b})]. \quad (9)$$

Then we conduct meta-test in auxiliary tasks to perform fine-grained fine-tuning in optimization direction.

$$\begin{aligned} \theta'_E &= \theta_E - lr \cdot \nabla_{\theta_E} \mathcal{L}_{FR_A}^{pri}(\theta_E), \\ x_{adv}^{att_b} &= G_{dec}(G_{enc}(x_{cov}^{att_a}), E_{adv}^{\theta'_E}(x_{cov}^{att_a}, att_b)), \\ \mathcal{L}_{FR_A}^{aux} &= \frac{\sum_{i=1 \cap i \neq A}^K w_i(t) (1 - \cos(FR_i(x_{target}), FR_i(x_{adv}^{att_b})))}{K - 1}, \end{aligned} \quad (10)$$

where we also employ a self-adaptive parameter w_i to balance the contributions of different surrogate models. Via this, it can prevent easily attackable surrogate models from dominating during training. We can obtain w_i from the following.

$$\begin{aligned} rate_i(t) &= \frac{Mean(\mathcal{L}_{FR_i}\{t-1\})}{Mean(\mathcal{L}_{FR_i}\{t-2\})}, i \in \{1, 2 \dots K\}, \\ w_i(t) &= \exp\left(\frac{\exp(rate_i(t))}{\sum_i^K \exp(rate_i(t))}\right), \end{aligned} \quad (11)$$

where $Mean(\mathcal{L}_{FR_i}\{t\})$ is the mean of \mathcal{L}_{FR_i} in t -th epoch.

Finally, the adversarial loss of ErasableMask is:

$$\mathcal{L}_{adv} = \max\left(\frac{1}{2K} \sum_i^K (\mathcal{L}_{FR_i}^{pri} + \mathcal{L}_{FR_i}^{aux}), \epsilon\right), \quad (12)$$

where ϵ is used to adjust the perturbation intensity.

C. Perturbation Erasion based on Information Injection

The reconstruction of protected faces is an ill-posed problem, as a single protected face $x_{adv}^{att_b}$ can potentially be reconstructed to numerous $x_{rec}^{att_b}$. Moreover, since the semantic perturbations in feature space permanently damage identifiable information in source faces, this makes it challenging for the restorer R to obtain enough information for perturbation erasion. To address this, ErasableMask injects clean-domain information during generation to maximize the amount of source information needed by R .

Specifically, a copy of G_{dec} is used by introducing an additional branch as shown in Fig. 3, where $x_{cov}^{att_a}$ is used as input to obtain the latent variable $z_{clean} = G_{enc}(x_{cov}^{att_a})$. Subsequently, the tuples (z_{clean}, att_b) and (z_{adv}, att_b) are input into G_{dec} , where feature fusion is performed after each layer's output and is controlled by weight γ . The restorer R is initialized with the same parameters and structures as G and is optimized utilizing the loss \mathcal{L}_{era} :

$$\begin{aligned} x_{rec}^{att_b} &= R(x_{adv}^{att_b}), \\ \mathcal{L}_{era} &= \sum_{n=1}^N \|x_{rec}^{att_b(n)} - x_{cov}^{att_b(n)}\|_2, \end{aligned} \quad (13)$$

where N is the number of training samples.

D. Robustness Enhancement and Curriculum Learning

In real-world facial privacy protection scenarios, online social platforms process uploaded images to comply with file storage and transmission standards. This processing significantly affects ErasableMask's adversarial and erasion performance. Therefore, after generating protected faces $x_{adv}^{att_b}$, ErasableMask incorporates a noise pool to enhance its robustness. The noise pool includes JPEG compression ($QF = 50$),

TABLE II
ASR AND ESR RESULTS AGAINST BLACK-BOX FR MODEL.

Datasets	Type	Scheme	Facenet		ArcFace		IRSE50		MobileFace		CosFace		IR152	
			ASR↑	ESR↑	ASR↑	ESR↑	ASR↑	ESR↑	ASR↑	ESR↑	ASR↑	ESR↑	ASR↑	ESR↑
CelebA-HQ	Without adversarial perturbation	Clean	0.45	-	0.0	-	0.50	-	0.05	-	0.0	-	1.65	-
		Attributes Modified	0.22	-	0.0	-	0.0	-	0.0	-	0.0	-	1.7	-
	Gradient-based	FGSM [29]	2.27	-	35.00	-	61.36	-	31.82	-	33.18	-	42.27	-
		PGD [30]	3.63	-	65.45	-	75.45	-	45.46	-	64.54	-	59.09	-
		Sibling Attack [31]	14.93	-	93.21	-	95.48	-	83.25	-	<u>92.31</u>	-	98.19	-
	Face-based	AdvFaces [6]	<u>35.00</u>	-	50.00	-	83.67	-	<u>91.33</u>	-	78.67	-	84.66	-
		SemanticAdv [11]	3.67	-	10.66	-	38.24	-	47.79	-	48.16	-	63.24	-
		GMAA [32]	16.04	-	44.79	-	59.91	-	13.85	-	50.59	-	61.29	-
	Erasable face-based	ErasableMask (ours)	64.00	96.67	<u>90.44</u>	98.22	<u>94.00</u>	89.33	92.22	94.89	93.33	98.89	<u>92.00</u>	88.00
	FFHQ	Without adversarial perturbation	0.0	-	0.0	-	0.0	-	0.0	-	0.0	-	2.0	-
			0.0	-	0.0	-	0.0	-	0.0	-	0.0	-	1.11	-
		Gradient-based	2.17	-	38.41	-	47.83	-	23.19	-	32.61	-	52.89	-
			5.04	-	68.34	-	62.58	-	34.53	-	63.31	-	65.46	-
			15.94	-	83.33	-	<u>88.41</u>	-	66.67	-	<u>85.51</u>	-	89.86	-
		Face-based	<u>25.60</u>	-	46.80	-	77.40	-	<u>68.80</u>	-	38.20	-	67.80	-
			5.88	-	21.33	-	31.98	-	15.07	-	22.06	-	35.66	-
			15.94	-	21.49	-	46.01	-	11.71	-	21.74	-	38.53	-
	Erasable face-based	ErasableMask (ours)	58.22	98.22	<u>81.78</u>	99.11	97.33	93.78	93.11	98.22	92.67	99.56	90.67	89.33

Gaussian noise ($Var = 0.003$), and Resizing transformations ($1/4$).

In the initial training stage, introducing all losses makes it challenging to learn an effective generation capability. To address this issue, we introduce a curriculum learning strategy that allows the model to gradually acquire generation and perturbation erasure capabilities over three stages.

In the first stage, we aim to develop a well-trained encoder G_{enc} and decoder G_{dec} . The loss function at this stage is:

$$\mathcal{L}_1 = \lambda_{rec}\mathcal{L}_{rec} + \lambda_{att}\mathcal{L}_{att}^G + \lambda_G\mathcal{L}_G. \quad (14)$$

In the second stage, we aim to ensure that \mathcal{L}_{adv} does not impair the model's ability to produce natural images. Thus, in this phase, we fix the parameters of the encoder G_{enc} and decoder G_{dec} , then introduce E_{adv} , which has the same structure and is initialized with the parameters of G_{enc} , to generate semantic perturbations. Additionally, we introduce R at this stage, initializing it with the parameters of the encoder G_{enc} and decoder G_{dec} . This stage allows E_{adv} and the R to be tightly coupled and can be trained end-to-end. The loss function of stage 2 is:

$$\mathcal{L}_2 = \lambda_{att}\mathcal{L}_{att}^G + \lambda_{rec}\mathcal{L}_{rec} + \lambda_G\mathcal{L}_G + \lambda_{adv}\mathcal{L}_{adv} + \lambda_{era}\mathcal{L}_{era} + \lambda_{perb}\mathcal{L}_{perb}. \quad (15)$$

Since erasing semantic perturbations and obtaining a non-adversarial example x_{rec}^{atta} from x_{adv}^{attb} is a challenging task, the third stage focuses on independently training the R to develop its ability to map from the adversarial domain to the clean domain. The loss function of stage 3 is:

$$\mathcal{L}_3 = \mathcal{L}_{era}. \quad (16)$$

V. EXPERIMENT

A. Experimental setting

1) *Implementation details and Dataset*: To maintain all losses on the same scale, we set the parameters λ_{att} , λ_{rec} ,

λ_G , λ_{adv} , λ_{era} , and λ_{perb} to 10, 150, 1, 200, 150, and 1 respectively. ErasableMask is trained with 200 epochs in the first stage, 100 epochs in the second stage, and 50 epochs in the third stage. The learning rate is set to 0.00002. We selected high-resolution datasets: CelebA-HQ [41], a high-quality facial image dataset containing approximately 30,000 images with a resolution of 512×512 , and FFHQ [42], a high-quality face dataset with over 70,000 images. To simulate real-world applications, we first use MTCNN [43] to extract and preprocess the facial regions within images. Due to computational constraints, each image in the dataset is downscale to a resolution of 256×256 . All experiments are conducted on RTX3090 GPU 24 GB \times 1.

2) *Practical Evaluation Metrics for Facial Privacy Protection*: We use **Attack Success Rate (ASR)** to evaluate the ability of facial privacy protection.

$$ASR = \frac{\sum_i^N 1(\cos[FR(x_{adv}), FR(x_{target})] > \tau_1)}{N}. \quad (17)$$

Where, $1(\cdot)$ denotes indicator function, ASR indicates that facial privacy protection is considered successful when the similarity between x_{adv} and x_{target} exceeds the threshold τ_1 . In this paper, τ_1 was set to 0.01 times the False Acceptance Rate (FAR) of the FR model.

To evaluate ErasableMask's performance of erasure, we propose the **Erasure Success Rate (ESR)** as a metric.

$$ESR = \frac{\sum_i^N 1(\cos[FR(x_{rec}), FR(x_{target})] < \tau_2)}{N}. \quad (18)$$

ESR indicates that ErasableMask has successfully reconstructed a clean example that does not disrupt face verification when the cosine similarity between x_{rec} and x_{target} is less than 0.1 times the False Acceptance Rate (FAR) of the FR model.

3) *Competitors*: To verify the performance of ErasableMask's black-box transferability, we implemented several benchmark adversarial attack schemes, including FGSM [29],

TABLE III
THE MEAN CONFIDENCE RETURNED FROM COMMERCIAL FR SYSTEMS.

Scheme	Aliyun Confidence		Face++ Confidence		Tencent Confidence		Mean Confidence	
Metric	Attack ↑	Erasion ↓	Attack ↑	Erasion ↓	Attack ↑	Erasion ↓	Attack ↑	Erasion ↓
Clean	4.65	-	39.92	-	8.66	-	17.74	-
FGSM	29.09	-	52.41	-	24.34	-	35.28	-
PGD	31.99	-	56.57	-	26.07	-	38.21	-
Sibling Attack	50.63	-	67.39	-	42.71	-	53.57	-
AdvFaces	43.38	-	70.65	-	47.72	-	53.92	-
SemanticAdv	30.19	-	55.05	-	29.12	-	38.12	-
GMAA	58.22	-	66.82	-	45.68	-	56.91	-
ErasableMask (ours)	67.01	5.11	78.19	42.72	69.06	10.15	72.60	23.92

For Attack, the higher (↑) the similarity confidence score between protected faces and target face returned by commercial systems, the better.

For Erasion, the lower (↓) the similarity confidence score between protected faces and target face returned by commercial systems, the better.

PGD [30], Sibling Attack [31], AdvFaces [6], Semanticadv [11], and GMAA [32]. FGSM and PGD are well-known schemes due to their strong adversarial capabilities, and we set the perturbation strength to $4/255$, considering noticeable noise introduced by additive perturbations. AdvFaces, Sibling Attack, Semanticadv and GMAA are recent schemes that generate adversarial examples specifically targeting FR models.

4) *Target models*: Following [13], we conducted extensive experiments and selected six FR models as white-box models: IR152 [44], IRSE50 [45], Facenet [46], Mobileface [47], ArcFace [47] based on IResNet100 [48], and CosFace [49] based on IResNet100. Three of these models were used as white-box models for training, while the remaining three were used as black-box models for evaluation. Subsequently, Face++ [50], Tencent [51] and Aliyun [52] were chosen as black-box commercial FR models to serve as target models. To evaluate transferability against black-box robust FR models, we fine-tuned ArcFace and CosFace on the public dataset LFW using adversarial training [53], achieving 99.28% and 99.35% accuracy on LFW dataset, respectively.

B. Comparison on Offline FR models

We benchmark against prior work [13], [14], [32] in Table. II, concentrating on evaluating ErasableMask’s transferability against black-box FR models. ErasableMask almost achieves optimal ASR among all competitors, surpassing all face-based schemes. Different from existing schemes, ErasableMask also shows strong transferability against FaceNet, with 30% higher than the second optimal.

Compared with existing facial protection schemes, ErasableMask offers a restorer that can perform perturbation erasion and obtain a clean-domain example. The perturbation erasion performance is also demonstrated in Table. II. The ESR results against all black-box FR models are almost close to 90%.

C. Comparison on Commercial FR systems

Another scenario is that unauthorized hackers choose commercial FR systems, like Aliyun, Tencent, and Face++. To simulate this, we employ commercial FR systems for face verification. We randomly select 100 examples for each scheme, then upload them and target face to platforms. We calculate the mean confidence rate and the results are demonstrated in

TABLE IV
THE ASR RESULTS AND ESR RESULT AGAINST ROBUST FR MODELS.

	Black-Box		Robust ArcFace		Robust CosFace	
Metric	ASR ↑	ESR ↑	ASR ↑	ESR ↑	ASR ↑	ESR ↑
Clean	0.0	-	0.0	-	-	-
FGSM [29]	2.73	-	1.36	-	-	-
PGD [30]	5.45	-	3.64	-	-	-
Sibling Attack [31]	30.32	-	25.34	-	-	-
AdvFaces [6]	36.0	-	61.0	-	-	-
SemanticAdv [11]	0.36	-	11.76	-	-	-
GMAA [32]	5.54	-	9.90	-	-	-
ErasableMask (ours)	79.78	100.0	81.33	98.44	-	-

Table. III. The mean confidence of ErasableMask is 9.79%, 7.54%, and 21.34% higher than the second higher scheme against Aliyun, Face++ and Tencent, respectively.

D. Comparison on Robust FR Models

In this section, we evaluate all competitors and ErasableMask against fine-tuned robust FR models. The results are demonstrated in Table. IV. ErasableMask outperforms all competitors with 79.78% against ArcFace and 81.33% against CosFace, respectively. Traditional gradient-based schemes exhibit the poorest performance against fine-tuned FR models. However, Sibling Attack employing attacking AR model as an auxiliary task exhibits higher robust performance than other gradient-based schemes. Among all face-based competitors, AdvFaces shows the highest ASR, mainly because AdvFaces generates additive perturbations rather than semantic perturbations. That is to say, semantic perturbation results in a poorer robustness compared with additive perturbation. However, ErasableMask overcomes the drawbacks of semantic perturbation, with over 70% higher than others.

E. Robustness Analysis

We evaluate robustness via applying JPEG($QF = 50$), Gaussian noise($Var = 0.003$), Resizing transformation($1/2$), Median Filter($Kernel = 5$), Random Rotate($angle \in [-30, 30]$), and Central Crop(224) to the protected faces in Table. V. ErasableMask demonstrates excellent protection and erasion capability in terms of ASR and ESR across. It outperforms almost all competitors in both white-box and black-box image processing methods, with rather high ASR. While it also shows excellent erasion capability in JPEG, Gaussian noise, Resizing transformation, Median Filter. Even though the erasion performance against Random Rotate and Central Crop shows less effectiveness, we think it is reasonable that TAs will not apply these methods to disrupt face verification.

F. Visualization and Image Quality

Fig. 4 demonstrates the protected faces generated by various schemes. Compared with gradient-based schemes, ours has no obvious pixel-level adversarial noise. Furthermore, we use L1 loss, Mean Square Error (MSE), Frechet Inception

TABLE V
ASR AND ESR RESULTS AFTER VARIOUS IMAGE PROCESSING OPERATIONS.

Processing	Type	Scheme	FaceNet		ArcFace		IRSE50		MobileFace		CosFace		IR152	
			ASR ↑	ESR ↑	ASR ↑	ESR ↑	ASR ↑	ESR ↑	ASR ↑	ESR ↑	ASR ↑	ESR ↑	ASR ↑	ESR ↑
Resize	Gradient-based	FGSM [29]	1.4	-	18.6	-	32.7	-	14.1	-	7.3	-	22.7	-
		PGD [30]	1.8	-	26.4	-	34.5	-	19.1	-	9.1	-	26.4	-
		Sibling Attack [31]	12.2	-	59.3	-	85.1	-	66.9	-	39.4	-	81.9	-
	Face-based	AdvFaces [6]	34.7	-	62.0	-	88.0	-	80.3	-	48.0	-	65.0	-
		SemanticAdv [11]	2.9	-	9.6	-	37.1	-	45.6	-	44.5	-	61.4	-
		GMAA [32]	8.2	-	18.4	-	48.1	-	8.4	-	31.3	-	47.3	-
Erasable face-based	ErasableMask (ours)	63.6	92.7	90.4	95.8	93.6	82.4	92.7	84.4	92.4	96.0	92.2	94.2	
JPEG	Gradient-based	FGSM [29]	2.3	-	16.8	-	35.9	-	14.1	-	7.3	-	20.9	-
		PGD [30]	3.6	-	24.5	-	38.2	-	20.9	-	10.9	-	23.6	-
		Sibling Attack [31]	14.0	-	71.5	-	91.9	-	71.9	-	57.0	-	89.6	-
	Face-based	AdvFaces [6]	33.7	-	45.3	-	72.7	-	82.0	-	47.0	-	69.3	-
		SemanticAdv [11]	4.0	-	4.0	-	36.4	-	42.3	-	24.6	-	53.7	-
		GMAA [32]	12.9	-	26.8	-	49.1	-	9.9	-	37.0	-	55.4	-
Erasable face-based	ErasableMask (ours)	63.8	91.3	90.2	95.8	93.6	81.8	92.7	86.0	92.9	93.8	91.6	76.4	
Gaussian noise	Gradient-based	FGSM [29]	2.3	-	23.6	-	53.2	-	20.5	-	17.7	-	33.2	-
		PGD [30]	3.6	-	41.8	-	62.7	-	28.2	-	29.1	-	46.4	-
		Sibling Attack [31]	14.5	-	87.3	-	95.0	-	79.2	-	85.9	-	97.7	-
	Face-based	AdvFaces [6]	31.3	-	47.3	-	81.7	-	87.6	-	71.6	-	80.7	-
		SemanticAdv [11]	2.6	-	2.9	-	29.0	-	26.8	-	28.3	-	47.4	-
		GMAA [32]	12.6	-	21.3	-	50.3	-	6.8	-	31.2	-	50.3	-
Erasable face-based	ErasableMask (ours)	63.7	93.1	88.2	96.0	92.9	80.7	91.6	86.9	89.3	94.9	91.1	81.6	
Median Filter	Gradient-based	FGSM [29]	1.8	-	18.6	-	37.3	-	15.5	-	6.4	-	22.3	-
		PGD [30]	2.7	-	29.1	-	41.8	-	21.8	-	9.1	-	23.6	-
		Sibling Attack [31]	13.6	-	59.7	-	83.7	-	64.3	-	38.5	-	83.7	-
	Face-based	AdvFaces [6]	35.3	-	59.3	-	87.3	-	74.0	-	31.0	-	55.0	-
		SemanticAdv [11]	1.5	-	7.7	-	38.2	-	43.0	-	43.0	-	58.8	-
		GMAA [32]	15.8	-	47.5	-	56.4	-	7.9	-	45.5	-	60.4	-
Erasable face-based	ErasableMask (ours)	63.3	92.7	90.4	96.0	93.1	83.8	92.7	86.7	92.9	96.0	92.4	78.7	
Random Rotate	Gradient-based	FGSM [29]	0.9	-	9.1	-	12.7	-	6.4	-	3.6	-	13.2	-
		PGD [30]	2.7	-	10.9	-	16.4	-	7.3	-	5.5	-	20.0	-
		Sibling Attack [31]	11.3	-	31.7	-	41.2	-	23.9	-	20.8	-	52.5	-
	Face-based	AdvFaces [6]	27.3	-	44.3	-	57.0	-	35.7	-	33.7	-	46.7	-
		SemanticAdv [11]	2.6	-	4.8	-	15.1	-	14.3	-	30.9	-	40.4	-
		GMAA [32]	10.9	-	30.7	-	39.6	-	4.9	-	43.6	-	48.5	-
Erasable face-based	ErasableMask (ours)	63.6	42.9	82.7	36.2	68.2	36.7	47.1	67.3	86.4	23.8	81.6	28.7	
Central Crop	Gradient-based	FGSM [29]	2.7	-	12.7	-	34.1	-	9.5	-	4.5	-	22.7	-
		PGD [30]	2.7	-	21.8	-	37.3	-	14.5	-	8.2	-	26.4	-
		Sibling Attack [31]	14.9	-	47.9	-	84.2	-	59.3	-	30.8	-	76.0	-
	Face-based	AdvFaces [6]	38.3	-	58.3	-	88.0	-	76.7	-	44.0	-	65.3	-
		SemanticAdv [11]	2.9	-	9.2	-	37.1	-	45.2	-	45.6	-	60.3	-
		GMAA [32]	15.8	-	44.6	-	60.4	-	11.9	-	49.5	-	62.4	-
Erasable face-based	ErasableMask (ours)	67.6	44.0	92.0	18.9	94.2	4.9	90.0	14.0	92.0	14.9	90.2	12.0	

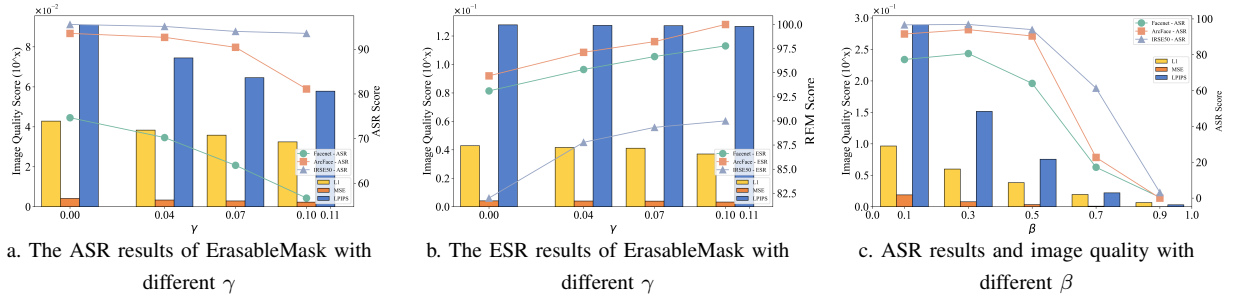
Fig. 5. ASR and ESR results for selection of different γ and β .

TABLE VII
ABLATION STUDY FOR META-AUXILIARY ATTACK. ASR RESULTS FOR
BLACK-BOX OFFLINE FR MODELS.

BlackBox	FaceNet	ArcFace	IRSE50	MobileFace	CosFace	IR152
w/o Meta-auxiliaryAttack	58.22	87.78	95.56	90.67	83.33	88.00
Meta-auxiliary Attack (ours)	64.00	90.44	94.09	92.22	93.31	92.00

adversarial loss \mathcal{L}_{adv} rapidly declined, and concurrently, the quality of protected faces significantly dropped. The model quickly identified the local optimum for the three white-box models, thereby demonstrating strong adversarial capabilities on these models. However, this rapid decrease led to challenges for ErasableMask in finding more general and robust features of FR models, ultimately resulting in suboptimal black-box performance under ensemble attacks.

2) *Without Information Injection*: In this section, we conduct experiments on different information injection weights γ . The results are demonstrated in Fig. 5 (a-b). As γ increases, the adversarial performance decreases while the image quality and erasure enhance. Particularly, when $\gamma = 0.1$, the ASR results against Facenet and ArcFace drop to 56.67 and 81.11, respectively, with a decrease over 15. The γ demonstrates a trade-off between adversarial and erasure performance of ErasableMask, which can improve the ASR results via decreasing γ and can improve the erasure performance through simply increasing γ . As shown in Fig. 5 (a-b), ErasableMask without information injection demonstrates the best ASR results, while exhibiting the worst erasure ability and image quality. Hence, ErasableMask is capable of utilizing various γ to cater to diverse real-world circumstances.

3) *ErasableMask with Different β* : In this section, we examine the selection of β . The experiment results are exhibited in Fig. 5 (c). The ASR results tend to drop smoothly before β decreases to 0.7, where the image quality enhances sharply. Especially, when $\beta = 0.5$, the image quality has a significant advantage over those whose $\beta \leq 0.3$, while the ASR results show little decrease against ArcFace and IRSE50. Although there is a decrease in ASR results of Facenet, it is reasonable considering the enhancement of image quality. When $\beta \geq 0.7$, image quality quickly increases with a significant drop in ASR results. As a result, we set $\beta = 0.5$ in our whole experiment.

VI. CONCLUSION AND LIMITATIONS

To address the limitations of existing facial privacy protection schemes, we propose ErasableMask, the first erasable

adversarial example-based facial privacy protection scheme. ErasableMask introduces an erasable adversarial mask on facial images, preventing malicious hackers from conducting face verification while offers erasure mechanism for TAs. Specifically, we first adopt a novel meta-auxiliary attack to boost black-box transferability via fine-grained balance the optimization and contributions of different surrogate FR models. Then we utilize a self-erasable strategy based on clean-domain information injection to erase semantic perturbations in protected faces. We also employ a three-stage curriculum learning strategy to solve the optimization conflicts between adversarial and erasure performance. Through extensive experiments on CelebA-HQ and FFHQ datasets, ErasableMask demonstrates the state-of-the-art transferability, robustness, and erasure performance. However, current quality evaluation metrics for adversarial examples do not apply to scenarios based on semantic perturbations, making it impractical to simply assess naturalness via similarity between the adversarial example and the original face.

VII. ACKNOWLEDGEMENT

The authors would like to thank the editor and reviewers for their careful reading and valuable comments. This research was supported by National Natural Science Foundation of China (No.62472325), and the Guangdong S&T Program under Grant 2024B0101010002, and the National Natural Science Foundation of China (No.U2436208, No.62372129), and the Project of Guangdong Key Laboratory of Industrial Control System Security (2024B1212020010).

REFERENCES

- [1] C. Ding and D. Tao, "Robust face recognition via multimodal deep face representation," *IEEE transactions on Multimedia*, vol. 17, no. 11, pp. 2049–2058, 2015.
- [2] Y. Zhong, W. Deng, H. Fang, J. Hu, D. Zhao, X. Li, and D. Wen, "Dynamic training data dropout for robust deep face recognition," *IEEE Transactions on Multimedia*, vol. 24, pp. 1186–1197, 2021.
- [3] B.-C. Chen, C.-S. Chen, and W. H. Hsu, "Face recognition and retrieval using cross-age reference coding with cross-age celebrity dataset," *IEEE Transactions on Multimedia*, vol. 17, no. 6, pp. 804–815, 2015.
- [4] J. Y. Choi, W. De Neve, K. N. Plataniotis, and Y. M. Ro, "Collaborative face recognition for improved face annotation in personal photo collections shared on online social networks," *IEEE Transactions on Multimedia*, vol. 13, no. 1, pp. 14–28, 2010.
- [5] M. Larson, Z. Liu, S. Brugman, and Z. Zhao, "Pixel privacy. increasing image appeal while blocking automatic inference of sensitive scene information," 2018.

- [6] D. Deb, J. Zhang, and A. K. Jain, "Advfaces: Adversarial face synthesis," in *2020 IEEE International Joint Conference on Biometrics (IJCB)*. IEEE, 2020, pp. 1–10.
- [7] S. Komkov and A. Petiushko, "Advhat: Real-world adversarial attack on arcface face id system," in *2020 25th international conference on pattern recognition (ICPR)*. IEEE, 2021, pp. 819–826.
- [8] Y. Dong, H. Su, B. Wu, Z. Li, W. Liu, T. Zhang, and J. Zhu, "Efficient decision-based black-box adversarial attacks on face recognition," in *proceedings of the IEEE/CVF conference on computer vision and pattern recognition*, 2019, pp. 7714–7722.
- [9] M. Sharif, S. Bhagavatula, L. Bauer, and M. K. Reiter, "Accessorize to a crime: Real and stealthy attacks on state-of-the-art face recognition," in *Proceedings of the 2016 acm sigsac conference on computer and communications security*, 2016, pp. 1528–1540.
- [10] L. Yang, Q. Song, and Y. Wu, "Attacks on state-of-the-art face recognition using attentional adversarial attack generative network," *Multimedia tools and applications*, vol. 80, pp. 855–875, 2021.
- [11] H. Qiu, C. Xiao, L. Yang, X. Yan, H. Lee, and B. Li, "Semanticadv: Generating adversarial examples via attribute-conditioned image editing," in *Computer Vision—ECCV 2020: 16th European Conference, Glasgow, UK, August 23–28, 2020, Proceedings, Part XIV 16*. Springer, 2020, pp. 19–37.
- [12] S. Jia, B. Yin, T. Yao, S. Ding, C. Shen, X. Yang, and C. Ma, "Adv-attribute: Inconspicuous and transferable adversarial attack on face recognition," *Advances in Neural Information Processing Systems*, vol. 35, pp. 34 136–34 147, 2022.
- [13] S. Hu, X. Liu, Y. Zhang, M. Li, L. Y. Zhang, H. Jin, and L. Wu, "Protecting facial privacy: Generating adversarial identity masks via style-robust makeup transfer," in *Proceedings of the IEEE/CVF conference on computer vision and pattern recognition*, 2022, pp. 15 014–15 023.
- [14] F. Shamsad, M. Naseer, and K. Nandakumar, "Clip2protect: Protecting facial privacy using text-guided makeup via adversarial latent search," in *Proceedings of the IEEE/CVF Conference on Computer Vision and Pattern Recognition*, 2023, pp. 20 595–20 605.
- [15] D. Liu, X. Wang, C. Peng, N. Wang, R. Hu, and X. Gao, "Adv-diffusion: imperceptible adversarial face identity attack via latent diffusion model," in *Proceedings of the AAAI Conference on Artificial Intelligence*, vol. 38, no. 4, 2024, pp. 2024–2033.
- [16] C. Hu, Y. Li, Z. Feng, and X. Wu, "Towards transferable attack via adversarial diffusion in face recognition," *IEEE Transactions on Information Forensics and Security*, 2024.
- [17] B. Yin, W. Wang, T. Yao, J. Guo, Z. Kong, S. Ding, J. Li, and C. Liu, "Adv-makeup: A new imperceptible and transferable attack on face recognition," in *International Joint Conference on Artificial Intelligence*, 2021.
- [18] L. Xiong, Y. Wu, P. Yu, and Y. Zheng, "A black-box reversible adversarial example for authorizable recognition to shared images," *Pattern Recognition*, vol. 140, p. 109549, 2023.
- [19] J. Liu, W. Zhang, K. Fukuchi, Y. Akimoto, and J. Sakuma, "Unauthorized ai cannot recognize me: Reversible adversarial example," *Pattern Recognition*, vol. 134, p. 109048, 2023.
- [20] J. Zhang, J. Wang, H. Wang, and X. Luo, "Self-recoverable adversarial examples: A new effective protection mechanism in social networks," *IEEE Transactions on Circuits and Systems for Video Technology*, vol. 33, no. 2, pp. 562–574, 2022.
- [21] Y. Xie, Y. Zhou, T. Wang, W. Wen, S. Yi, and Y. Zhang, "Reversible gender privacy enhancement via adversarial perturbations," *Neural Networks*, vol. 172, p. 106130, 2024.
- [22] Z. Yin, L. Chen, W. Lyu, and B. Luo, "Reversible attack based on adversarial perturbation and reversible data hiding in yuv colorspace," *Pattern Recognition Letters*, vol. 166, pp. 1–7, 2023.
- [23] S. Liu, A. Davison, and E. Johns, "Self-supervised generalisation with meta auxiliary learning," *Advances in Neural Information Processing Systems*, vol. 32, 2019.
- [24] H. Chen, X. Wang, Y. Zhou, Y. Qin, C. Guan, and W. Zhu, "Joint data-task generation for auxiliary learning," *Advances in Neural Information Processing Systems*, vol. 36, 2024.
- [25] C. Finn, P. Abbeel, and S. Levine, "Model-agnostic meta-learning for fast adaptation of deep networks," in *International conference on machine learning*. PMLR, 2017, pp. 1126–1135.
- [26] R. Shao, X. Lan, and P. C. Yuen, "Regularized fine-grained meta face anti-spoofing," in *Proceedings of the AAAI conference on artificial intelligence*, vol. 34, no. 07, 2020, pp. 11 974–11 981.
- [27] Z. Jia, H. Fang, and W. Zhang, "Mbrs: Enhancing robustness of dnn-based watermarking by mini-batch of real and simulated jpeg compression," in *Proceedings of the 29th ACM international conference on multimedia*, 2021, pp. 41–49.
- [28] X. Wang, Y. Chen, and W. Zhu, "A survey on curriculum learning," *IEEE transactions on pattern analysis and machine intelligence*, vol. 44, no. 9, pp. 4555–4576, 2021.
- [29] I. J. Goodfellow, "Explaining and harnessing adversarial examples," *arXiv preprint arXiv:1412.6572*, 2014.
- [30] A. Madry, A. Makelov, L. Schmidt, D. Tsipras, and A. Vladu, "Towards deep learning models resistant to adversarial attacks," in *6th International Conference on Learning Representations, ICLR 2018, Vancouver, BC, Canada, April 30 - May 3, 2018, Conference Track Proceedings*. OpenReview.net, 2018.
- [31] Z. Li, B. Yin, T. Yao, J. Guo, S. Ding, S. Chen, and C. Liu, "Sibling-attack: Rethinking transferable adversarial attacks against face recognition," in *Proceedings of the IEEE/CVF Conference on Computer Vision and Pattern Recognition*, 2023, pp. 24 626–24 637.
- [32] Q. Li, Y. Hu, Y. Liu, D. Zhang, X. Jin, and Y. Chen, "Discrete point-wise attack is not enough: Generalized manifold adversarial attack for face recognition," in *Proceedings of the IEEE/CVF Conference on Computer Vision and Pattern Recognition*, 2023, pp. 20 575–20 584.
- [33] Y. Dong, F. Liao, T. Pang, H. Su, J. Zhu, X. Hu, and J. Li, "Boosting adversarial attacks with momentum," in *Proceedings of the IEEE conference on computer vision and pattern recognition*, 2018, pp. 9185–9193.
- [34] Z. Xiao, X. Gao, C. Fu, Y. Dong, W. Gao, X. Zhang, J. Zhou, and J. Zhu, "Improving transferability of adversarial patches on face recognition with generative models," in *Proceedings of the IEEE/CVF conference on computer vision and pattern recognition*, 2021, pp. 11 845–11 854.
- [35] X. Yang, Y. Dong, T. Pang, H. Su, J. Zhu, Y. Chen, and H. Xue, "Towards face encryption by generating adversarial identity masks," in *Proceedings of the IEEE/CVF International Conference on Computer Vision*, 2021, pp. 3897–3907.
- [36] Y. Zhong and W. Deng, "Towards transferable adversarial attack against deep face recognition," *IEEE Transactions on Information Forensics and Security*, vol. 16, pp. 1452–1466, 2020.
- [37] N. Carlini and D. Wagner, "Towards evaluating the robustness of neural networks," in *2017 IEEE Symposium on Security and Privacy (SP)*. IEEE, 2017, pp. 39–57.
- [38] X. Wei, Y. Guo, J. Yu, and B. Zhang, "Simultaneously optimizing perturbations and positions for black-box adversarial patch attacks," *IEEE transactions on pattern analysis and machine intelligence*, vol. 45, no. 7, pp. 9041–9054, 2022.
- [39] M. Li, J. Wang, H. Zhang, Z. Zhou, S. Hu, and X. Pei, "Transferable adversarial facial images for privacy protection," *arXiv preprint arXiv:2408.01428*, 2024.
- [40] Z. He, W. Zuo, M. Kan, S. Shan, and X. Chen, "Attgan: Facial attribute editing by only changing what you want," *IEEE transactions on image processing*, vol. 28, no. 11, pp. 5464–5478, 2019.
- [41] T. Karras, "Progressive growing of gans for improved quality, stability, and variation," *arXiv preprint arXiv:1710.10196*, 2017.
- [42] T. Karras, S. Laine, and T. Aila, "A style-based generator architecture for generative adversarial networks," in *Proceedings of the IEEE/CVF conference on computer vision and pattern recognition*, 2019, pp. 4401–4410.
- [43] K. Zhang, Z. Zhang, Z. Li, and Y. Qiao, "Joint face detection and alignment using multitask cascaded convolutional networks," *IEEE signal processing letters*, vol. 23, no. 10, pp. 1499–1503, 2016.
- [44] K. He, X. Zhang, S. Ren, and J. Sun, "Deep residual learning for image recognition," in *Proceedings of the IEEE conference on computer vision and pattern recognition*, 2016, pp. 770–778.
- [45] J. Hu, L. Shen, and G. Sun, "Squeeze-and-excitation networks," in *Proceedings of the IEEE conference on computer vision and pattern recognition*, 2018, pp. 7132–7141.
- [46] F. Schroff, D. Kalenichenko, and J. Philbin, "Facenet: A unified embedding for face recognition and clustering," in *Proceedings of the IEEE conference on computer vision and pattern recognition*, 2015, pp. 815–823.
- [47] J. Deng, J. Guo, N. Xue, and S. Zafeiriou, "Arcface: Additive angular margin loss for deep face recognition," in *Proceedings of the IEEE/CVF conference on computer vision and pattern recognition*, 2019, pp. 4690–4699.
- [48] I. C. Duta, L. Liu, F. Zhu, and L. Shao, "Improved residual networks for image and video recognition," in *2020 25th International Conference on Pattern Recognition (ICPR)*. IEEE, 2021, pp. 9415–9422.
- [49] H. Wang, Y. Wang, Z. Zhou, X. Ji, D. Gong, J. Zhou, Z. Li, and W. Liu, "Cosface: Large margin cosine loss for deep face recognition," in *Proceedings of the IEEE conference on computer vision and pattern recognition*, 2018, pp. 5265–5274.
- [50] MEGVII, "In <https://www.faceplusplus.com.cn/>," 2021.
- [51] T. Cloud, <https://cloud.tencent.com/document/product/867>.

- [52] Aliyun, “<https://cn.aliyun.com/>,” 2019.
- [53] A. Madry, “Towards deep learning models resistant to adversarial attacks,” *arXiv preprint arXiv:1706.06083*, 2017.
- [54] M. Heusel, H. Ramsauer, T. Unterthiner, B. Nessler, and S. Hochreiter, “Gans trained by a two time-scale update rule converge to a local nash equilibrium,” *Advances in neural information processing systems*, vol. 30, 2017.
- [55] R. Zhang, P. Isola, A. A. Efros, E. Shechtman, and O. Wang, “The unreasonable effectiveness of deep features as a perceptual metric,” in *CVPR*, 2018.